Impact of High-Intensity Ultrasound Waves on structural, functional, thermal and rheological properties of rice flour and its biopolymers structural features

Antonio J. Vela; Marina Villanueva; Ángela García Solaesa; Felicidad Ronda*

Department of Agriculture and Forestry Engineering, Food Technology, College of Agricultural and Forestry Engineering, University of Valladolid, Spain
**Corresponding author. E-mail: fronda@iaf.uva.es*

Abstract

Physical modifications of flours are an environment-friendly technology receiving increasing attention for widening the range of utilization of these raw materials. Rice flour was modified with ultrasound treatments at a frequency of 24 kHz and varying treatment time (2 to 60 min) and flour concentration (5 to 30%) in the dispersion. The effect of the modification was measured in the flours' physical, functional, pasting and rheological properties. Particle size of treated samples was reduced, and particle's disruption was observed by SEM; this had an impact on the water absorption ability, as shown by a sharp increase of swelling power. The thermal properties showed a significant reduction of gelatinization enthalpy, as well as narrowing of the gelatinization temperature range, characteristic of better packed starch crystalline structures after sonication. Modified patterns in starch and proteins were obtained with XRD and FTIR, which indicated impact to their crystalline and amide I secondary structures as a consequence of ultrasonication. Pasting profiles were found to be reduced with increasing treatment time, while higher concentrations did not significantly change the modification achieved. The pasting temperature was found to be significantly increased in all treated samples. Ultrasound treatment led to gels with higher strength, obtaining lower values of tan δ with increasing sonication time and flour concentration. Ultrasound allowed the modulation of rice flour functionality, being the effect independent on the concentration of the treated flour dispersion, up to 30%, and increased by treatment time up to 10 minutes; for longer treatments not many differences were found.

Keywords: Rice flour; High-Intensity Ultrasound Treatment; Thermal properties; Pasting properties; Biopolymers structure; Gel Rheological properties.

1. Introduction

Flours are among the main sources of carbohydrates in human consumption, commonly used in the food industry as thickener and bulking agents (Iida, Tuziuti, Yasui, Towata, & Kozuka, 2008). Rice flour is considered an interesting cereal grain in the gluten-free market because it can be used to replace wheat in an easier way than other cereals or pseudocereals, mainly because of its functional properties such as having a bland taste, its white color, digestibility and low allergenicity (Villanueva, Harasym, Muñoz, & Ronda, 2018; Wu, Chen, Li, & Wang, 2010). However, native flours have a limited industrial range of use due to their natural characteristics that limit their functionality, then modifications are applied to alter their physicochemical properties. The modification methods can be genetic, mechanical, chemical, enzymatic or physical (Zheng et al., 2013; Zhu, 2015). Physical modifications stand out for being an environment-friendly technology, and involving a reduced use of chemicals and processing time (Amini, Razavi, & Mortazavi, 2015). Ultrasounds (US) have been used in recent years in the food industry as a resource to generate physical modifications (Chemat, Zill-E-Huma, & Khan, 2011). Ultrasounds are acoustic waves above the human audible threshold, that can be classified in low intensity-high frequency US (>1MHz) and high intensity-low frequency US (20 - 100 kHz) (Zhu & Li, 2019). Sonication treatments are applied in a liquid-solid system, mostly using water as the medium (Zhu, 2015).

Ultrasound treatments are capable of altering the structure of flour's main biopolymers, starches and proteins, by acoustic cavitation and the generation of free radicals, but in the case of high intensity-low frequency US the amount of free radicals generated is low (Ashokkumar, 2015; O'Sullivan, Park, Beevers, Greenwood, & Norton, 2017). The acoustic energy of ultrasound is not absorbed by the treated molecules, so it is transformed to a chemically usable form through the cavitation phenomenon (Zhu, 2015). Acoustic cavitation is the cyclic generation and collapse of tiny bubbles in the aqueous medium as a result of pressure variation and US waves passing through. The cyclic collapsing of the bubbles results as water micro-jets shooting onto the particle's surface, leading to local rises of temperatures and very high shearing forces, that cause mechanical damage to the sonicated matrix, detected as cracks, pitting and irregular surfaces, leading to a reduction of the particle size and molecular weight (Ashokkumar, 2015; Bai, Hébraud, Ashokkumar, & Hemar, 2017; Mir, Riar, & Singh, 2019; O'Sullivan et al., 2017; Zheng et al., 2013). The effect of the physical forces derived from cavitation is very homogeneous throughout the dispersions sonicated in water, since water has a high surface tension which makes a very effective medium for

cavitation (Ashokkumar, 2015; Knorr, Zenker, Heinz, & Lee, 2004). The effect of US treatments on starch depends on variables such as the sonication frequency and power, time and temperature of the treatment, and botanical origin of the sample (Zhu, 2015).

In the cereal science field, research has been mainly focused on the effect of US treatments on starches from diverse botanical origins such as corn (Amini et al., 2015; Flores-Silva et al., 2017; Jambrak et al., 2010), wheat (Sujka, 2017), potato (Bai et al., 2017; Degrois, Gallant, Baldo, & Guilbot, 1974), sweet potato (Zheng et al., 2013), maize (Bel Haaj, Magnin, Pétrier, & Boufi, 2013; Luo et al., 2008), barley (Kaur & Gill, 2019), tapioca (Iida et al., 2008), plantain (Carmona-García et al., 2016) and rice (Yu et al., 2013; Zuo, Knoerzer, Mawson, Kentish, & Ashokkumar, 2009), while less research has been centered on flours. It is also important to generate knowledge of the effect that US treatments have on modifying flours since they are more complex systems widely used as a food ingredient, having the advantage of being cheap and nutritious. According to our knowledge, the study of their effect on rice flour is unexplored. The aim of this research was to investigate the effect of US treatments of 24 kHz frequency on functional, pasting, rheological and physical properties of rice flour, as a function of treatment time and flour concentration in the dispersion.

2. Materials and methods

2.1 Rice Flour

The rice flour used in this experiment was supplied by Emilio Esteban SA (Valladolid, Spain). The flour was stored at 4°C until it was used. The moisture content was 13.67%, protein 6.60%, fat 2.06% and ash 0.34% (data provided by the manufacturer). This native flour was used without any processing as the control in the study. Rice flour dispersions were prepared for the treatments by suspending the proper amount of flour in distilled water to achieve the desired concentration. All concentrations are given in g dry flour/100 g of dispersion.

2.2 Ultrasound Treatment

The ultrasound generator consisted of Hielscher UP400St sonicator (Hielscher Ultrasonics, Germany) equipped with S24d22D titanium tip working at a constant frequency of 24 kHz with a maximum output power of 180W, at 80% on-off pulse. The rice dispersions (400g) were treated in a glass jacket containing circulating water from a water bath to set the target temperature at 20ºC and keep it constant during the treatment. When the effect of the

treatment time was studied, the concentration of rice flour in the dispersion was fixed at 10g/100g while the time varied from 2 to 60 min (see Table 1). For evaluating the effect of the flour concentration, the treatment time was maintained at 60 min and the concentration of the rice flour in the dispersion varied from 5 to 30g/100g (Table 1). All dispersions were stirred during the treatment to avoid sedimentation and to ensure a homogenous temperature. After sonication samples were freeze-dried with Genesis Pilot Lyophilizer (SP Industries Inc, Warminster, USA). All samples were sieved to <250µm and stored at 4°C.

Table 1. Sonication conditions and ID of treated samples used in the study.

Sample	Treatment time (min)	Concentration (g solids/100g)
Control (native)	0	--
TIM-2	2	10
TIM-5	5	10
TIM-10	10	10
TIM-20	20	10
TIM-40	40	10
TIM-60	60	10
CON-5	60	5
CON-10	60	10
CON-20	60	20
CON-30	60	30

TIM-60 and CON-10 are samples with the exact same experimental conditions

2.3 Particle size distribution

The particle size distribution of the studied samples was stablished using a Mastersizer 3000 laser diffraction particle size analyzer (Malvern Instruments Ltd, UK). Results are expressed in median diameter (D_{50}) and ((D_{90}-D_{10})/D_{50}) as described in Abebe, Collar, & Ronda (2015). All samples were measured in triplicate.

2.4 Scanning Electron Microscopy (SEM)

A Quanta 200FEG scanning electron microscope (FEI, Oregon, U.S.A.) was used to study the surface microstructure of the samples, equipped with an X-ray detector, which allowed

the analysis of the samples without prior metallization. The visualizations were performed with an accelerating voltage between 3 and 5 keV in low vacuum mode using a secondary electron detector at different magnifications. Representative micrographs were selected for illustrative purposes.

2.5 Starch Damage

The percentage of damaged starch was measured following the AACC Official Method 76-31.01 (AACC, 2014) using a Megazyme starch damage kit (K-SDAM). The results were expressed as g/100g of the sample on dry basis. All samples were evaluated in triplicate.

2.6 Hydration properties of flour

Water absorption capacity (WAC) was measured following the centrifugation method described by Abebe, Collar & Ronda (2015). The results were expressed in g H_2O/g flour dry matter. Water absorption index (WAI), water solubility index (WSI) and swelling power (SP) were determined with slight modifications of the method indicated by Abebe et al., (2015). A sample of 2g was dispersed in 40mL of distilled water in 50mL centrifuge tubes. Samples were boiled for 15 min and cooled down to room temperature before being centrifuged at 3000xg (Thermo Fisher Scientific, Waltham, U.S.A.) for 10 min. The supernatant was poured in a previously weighed evaporating capsule to determine its solid content, and the sediment was weighed. The weight of the soluble solids was determined by evaporating the water from the supernatant overnight at 110°C. WAI was expressed in g sediment/g flour dry matter (dm), WSI in g soluble solids/100 g flour dm and SP in g sediment/g of insoluble solids in flour. All results were referred to dry matter to avoid the effect of different water content in the samples.

2.7 X-Ray diffraction (XRD)

XRD patterns were obtained using a Bruker-D8-Discover-A25 diffractometer (Bruker AXS, Rheinfelden, Germany) equipped with a Cu-Kα radiation (λ = 0.154 nm) at a voltage of 40 kV and a current of 40 mA. Before measurement all samples were equilibrated to 15% humidity using a saturated humidity ICP260 incubator at 15°C (Memmert GmbH, Germany). The radiation intensities of the equilibrated samples were measured in the range of 5° to 40° of 2θ diffraction angle, with a scan step size of 0.02°, receiving slit width of 0.02nm, scatter slit width of 2.92°, divergence slit width of 1° and a rate of 1.2°/min. The crystallinity of the

samples was calculated as the ratio between the reduced peak area assigned to the crystalline part and the total area using peak-fitting software DifracEVA with PDF2-2004 and Crystallography Open Database.

2.8 Fourier Transform Infrared Spectroscopy (FTIR)

FTIR spectra of the samples were recorded using a FT-IR Nicolet iS50 spectrophotometer (Thermo Fisher Scientific, U.S.A.) coupled with an attenuated total reflectance (ATR) device equipped with a diamond crystal. All samples were equilibrated at a humidity of 15% (as described in 2.7). All measurements were performed in duplicate in the wavenumber range of 600-4000cm^{-1} with a resolution of 4cm^{-1} and accumulation of 64 scans. All spectra were normalized using OMNIC software (Thermo Fisher Scientific, U.S.A.). Amide I bands (1700-1600 cm^{-1}) were analyzed using PeakFit 4.12 (SeaSolve Software Inc., USA). The individual components of deconvolved curves were determined by iterative fitting procedure that assumed Gaussian band shapes. Positions of the band centers were evaluated from second derivative analysis. The relative areas of these bands were used to estimate the percentage of secondary structural features: β-turns (1700-1660 cm^{-1}), α-helix (1658-1650 cm^{-1}), random coil (1650-1640 cm^{-1}) and β-sheet (1640-1600 cm^{-1}) (Byler & Susi, 1986; Zhang et al., 2018).

2.9 Differential scanning calorimetry (DSC)

The samples' thermal properties were measured using a DSC3 calorimeter (Mettler Toledo, Spain). The sample (~6 mg) was weighed in a 40 μL aluminum pan. The corresponding amount of distilled water was added to reach a solid concentration of ~30% w/w. The pans were sealed and allowed to rest for 30 min at room temperature before performing the measurement. The scan was performed from 0 to 110°C at a rate of 5°C/min, using an empty sealed pan as reference. The values measured were onset (T_O), peak (T_P) and endset (T_E) temperatures (°C) and the enthalpy of gelatinisation (ΔH) (J/g flour dm). The gelatinized samples were kept in the pans at 4±2°C and after 7 days they were measured again with the same method to study their retrogradation transition. All measurements were performed in duplicate.

2.10 Pasting analysis

The pasting properties of the samples were studied using a Kinexus Pro+ rheometer (Malvern Instruments Ltd, UK) equipped with a starch pasting cell geometry following the AACC

International Method 76-21.02 Standard 2 (AACC, 2017). The samples (3.50g on a moisture basis of 14%) were transferred to the test canister and 25.0±0.1mL of distilled water were added. The paddle speed was set at 160 rpm. The pasting temperature (PT), peak viscosity (PV), trough viscosity (TV), breakdown viscosity (BV), final viscosity (FV) and setback viscosity (SV), were calculated using the rSpace for Kinexus software (Malvern Instruments Ltd, UK). Samples were measured in duplicate.

2.11 Rheological properties of gels

The dynamic oscillatory tests were performed using a Kinexus Pro+ rheometer (Malvern Instruments Ltd, UK) with serrated parallel plate geometry (40 mm diameter) and a working gap of 1 mm. The gel samples were prepared following the protocol described in section 2.10 and left on the bottom plate to rest for 5 min to allow relaxation. Stress sweeps were performed from 0.1 to 100 Pa at a constant frequency of 1Hz. Frequency sweeps were performed from 10 to 1 Hz, at 1.0 Pa, within the linear viscoelastic region (LVR). The tests were carried out at constant temperature (25 °C) controlled with a Peltier KNX2002 C25P plate (Malvern Instruments Ltd, UK). The data obtained from frequency sweeps were adjusted to potential equations as described by Ronda, Villanueva, & Collar (2014). Tests were carried out in duplicate.

2.12 Statistical analysis

Analysis of variance (ANOVA) was carried out using Statgraphics Centurion v.6 (Bitstream, Cambridge, MN, U.S.A.). Tukey's honest significant difference (HSD) test was used to evaluate significant differences between samples at $p \leq 0.05$.

3. Results and Discussion

3.1 Morphology and particle size of samples

Scanning electron micrographs of selected flours are illustrated in Fig. 1. The images of native flour showed the characteristic morphology of rice flour, which are polygonal compact structure of starch granules packed very tightly in the cell, being entwined with globular protein bodies and lipids (Villanueva, Harasym, et al., 2018). In all treated samples it was observed that sonication caused a general disruption of these structures (see Fig. 1 – B2-C2-D2-E2). In rice starch, it has been reported that ultrasound leads to the formation of cracks and pores (Yang et al., 2019), which were not observed in rice flour, probably as

consequence of the protective effect that the remaining components of flour (mainly proteins and lipids) have on starch granules. Subsequent magnifications revealed structural fragmentation (higher amount of small size particles and loosen starch granules), and changes in the surface shape of the macrostructures, being more rugged and uneven after treatment, with starch granules having a wider exposed area in the surface, caused by the influence that shear forces of cavitation have on the granules' surface (Luo et al., 2008).

Granulation and uniformity of particle size have long been assumed to be important factors affecting the processing performance of flours. The particle size distribution of the treated samples showed significant changes compared to the native flour (see Supplementary Fig. 1). While the control sample showed a small percentage of particles in the range of 1 to 10μm, all ultrasonicated samples presented a marked percentage increase in this range, and showed a clear bimodal particle size distribution. The results of the median diameter (D_{50}) and size distribution ((D_{90}-D_{10})/D_{50}) (Table 2) also confirmed that sonication led to a reduction of particle size. Two minutes of sonication reduced D_{50} from 123 to 65 μm; five minutes decreased it up to 49 μm. Longer treatment times did not result in additional reduction. The effect of the flour concentration on the resulting particle size distribution was also significant ($p<0.05$). The greatest effect was obtained for the lowest flour concentration (CON-5) that led to a reduction of 72% in D_{50} with respect to the control flour. The effect was slightly diminished at higher concentrations with decreases in D_{50} of 52-58% for CON-10 to CON-30 samples. This reduction observed in every sonicated sample can be explained as a fragmentation caused by the cavitation phenomenon, given that collapsing bubbles generate material fatigue, followed by a gradual tearing off of microscopic particles (Degrois et al., 1974). It is believed that the fragmentation of the starch chains induced by sonication does not happen in a random manner, and there is a limit to that degradation and once that limit is reached, no further chain scission happens (Czechowska-Biskup, Rokita, Lotfy, Ulanski, & Rosiak, 2005). The decreased fragmentation in flours treated at higher concentration can be the result of a reduction of acoustic energy, due to a change of medium impedance (Amini et al., 2015; Degrois et al., 1974).

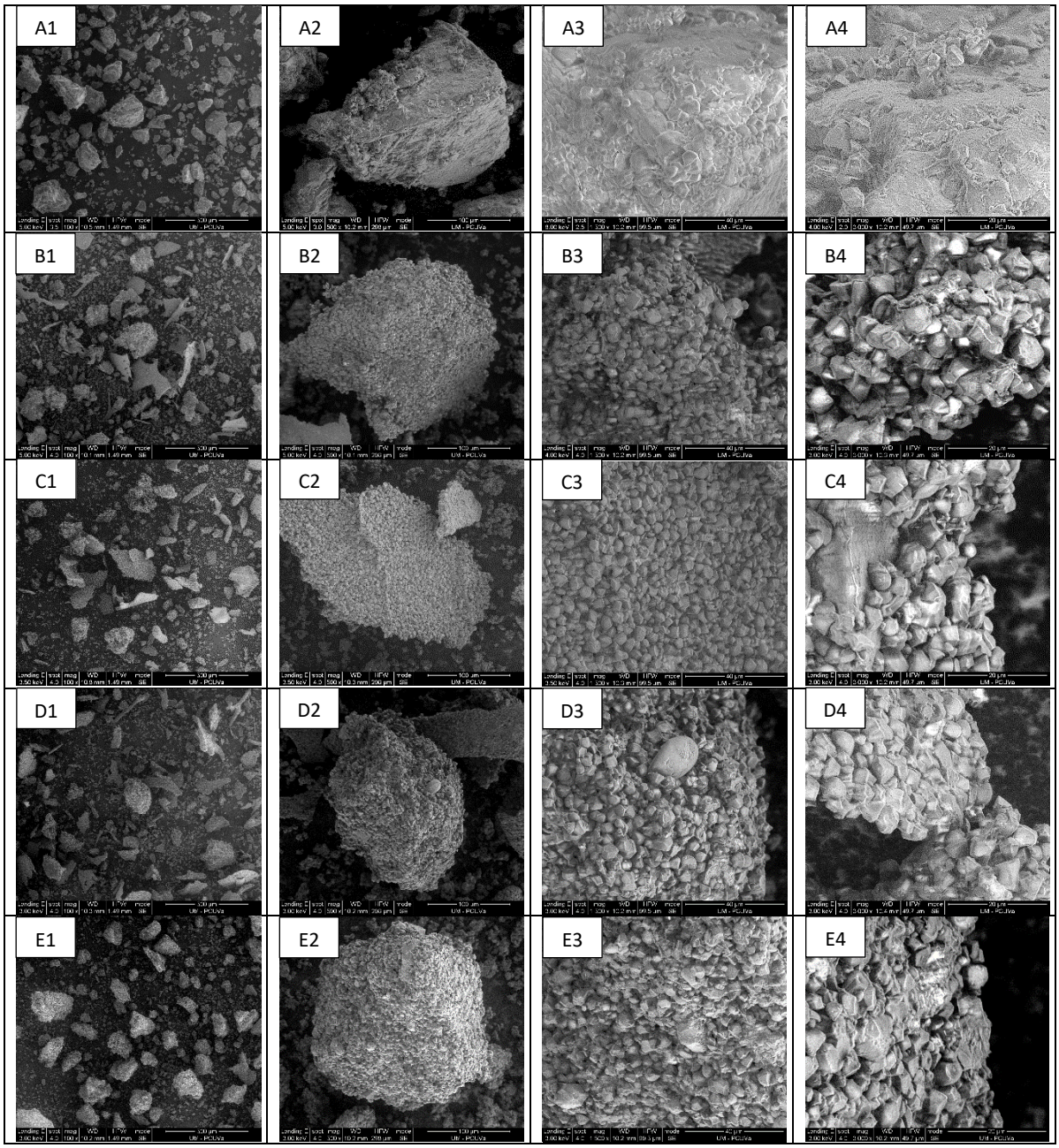

Figure 1. SEM images of (A) Control flour, (B) TIM-10, (C) TIM-60 (CON-10), (D) CON-5 and (E) CON-30 at a magnification of (1) 100x, (2) 500x, (3) 1500x and (4) 3000x.

Table 2. Particle size distribution, content of damaged starch and hydration properties of the sonicated flours and the control flour.

Sample	D_{50} (μm)	$(D_{90}-D_{10})/ D_{50}$	Starch damage (g/100g)	WAC (g/g)	WAI (g/g)	WSI (g/100g)	SP (g/g)
Effect of treatment time							
Control	123.0f	1.884a	6.9a	1.13ab	7.1a	4.7d	7.4a
TIM-2	64.7e	2.756b	-----	1.21c	11.2b	6.0e	12.0b
TIM-5	49.1a	3.373f	-----	1.19bc	14.4c	3.9c	15.0c
TIM-10	54.6b	3.419g	7.0ab	1.12ab	15.7d	3.3abc	16.3de
TIM-20	60.8d	2.811c	7.3abc	1.09a	15.6d	3.1ab	16.1d
TIM-40	55.9c	3.085e	7.5bc	1.08a	16.6e	2.7a	17.1ef
TIM-60	55.5c	2.971d	7.8c	1.09a	16.6e	3.4bc	17.2f
SE	0.1	0.002	0.1	0.02	0.2	0.1	0.2
Analysis of variance and significance (p-values)							
	***	***	**	***	***	***	***
Effect of flour concentration							
Control	123.0e	1.884a	6.9a	1.13bc	7.1a	4.7c	7.4a
CON-5	35.2a	4.404e	7.7b	1.14c	17.4c	2.6a	17.9c
CON-10	55.5c	2.971b	7.8b	1.09ab	16.6b	3.4b	17.2b
CON-20	52.2b	3.922d	7.6ab	1.07a	16.9bc	3.2b	17.4bc
CON-30	59.6d	3.709c	7.5ab	1.10abc	16.3b	3.4b	16.9b
SE	0.1	0.004	0.2	0.01	0.1	0.1	0.1
Analysis of variance and significance (p-values)							
	***	***	*	**	***	***	***

D_{50}: median diameter; $(D_{90}-D_{10})/D_{50}$: size dispersion. WAC = Water absorption capacity. WAI = Water absorption index.
WSI = Water solubility index. SP = Swelling power. Starch damage, WAC, WAI, WSI, SP are referred to dry matter.
SE: Pooled standard error from ANOVA. The different letters in the corresponding column within each studied factor indicate statistically significant differences between means at $p < 0.05$.
Analysis of variance and significance: *** $p < 0.001$. ** $p < 0.01$. * $p < 0.05$. ns: not significant.

3.2. Starch Damage

The damaged starch determined in sonicated and control flours is shown in Table 2. The results confirm a significant disruptive impact of ultrasonication on flour particles, moderately dependent on treatment time and flour concentration. The content of damaged starch

increased with sonication time, from 6.9% (native flour) to 7.8% (TIM-60). When sonicating during the same period of time different flour concentrations, the results showed similar effect within samples, where only CON-5 and CON-10 were significantly different than the control sample, leading to the conclusion that higher concentrations do not limit the impact that cavitation has over the samples' starch. The observed results go in line with the smaller particle size obtained in all treated samples, referring to a general disruption of flour macrostructures. Previous works demonstrated the significant negative correlation between the flour particle size and its starch damage content (Abebe et al., 2015).

3.3 Hydration properties

The WAC, WAI, WSI and SP values of native and treated samples are shown in Table 2. The WAC showed a slight increase at the shortest treatment times (2 and 5 min) and a later decrease at longer times. WAC is mainly determined by the hydrophilic parts in proteins and carbohydrates (Jitngarmkusol, Hongsuwankul, & Tananuwong, 2008). Ultrasound treatment can dissociate proteins and modify their secondary structure affecting their water binding sites (Kumar, Sharma, & Singh, 2017). The flour particle size also may affect the WAC of flour (Abebe &Ronda 2015). In any case, changes in WAC as result of the treatment were not of high quantitative importance. However, the WAI, SP and WSI were strongly affected by sonication and the following processing of the samples to restore the flours' granular structure. WAI and SP showed a sharp increase in all treated samples, with a slight increasing trend with treatment time, reaching in TIM-40 and TIM-60 samples a value 133% greater than that of the native flour. The sonication was more effective at the lowest flour concentration (CON-5), being 138% higher than the control in both WAI and SP. However, no significant differences were found in both parameters for concentrations of 10 to 30%. These general increases can be related to the physical damage suffered by the treated flour as was explained in previous sections (3.1 and 3.2). Other researchers have determined a significant increase in SP after sonication of starches from sources as corn (Amini et al., 2015; Jambrak et al., 2010), barley (Kaur & Gill, 2019), wheat and rice (Sujka & Jamroz, 2013). These changes have been attributed to modifications caused to the starch granule structure, in the degree of association between chains (Kaur & Gill, 2019), the structural arrangement of the amylose and amylopectin (Luo et al., 2008) and the breakdown of intermolecular bonds (Luo et al., 2008). It is believed that the increased surface area of starch granules in treated flours (accumulation of smaller particles as well as increased exposed area), as well as dissociation

of proteins that increases their water binding sites, allow an easier interaction with water, achieving a higher water uptake and retention (Amini et al., 2015; Kaur & Gill, 2019).

WSI decreased in all treated samples, with the sole exception of TIM-2, where a slight increase was observed. This behavior could be explained by a modification of the amylose/amylopectin ratio after sonication (Zheng et al., 2013). Flores-Silva et al. (2017) and Huang, Li, & Fu (2007) reported a disruption of amylose chains at short ultrasonication times (3 and 4 min) mainly from the outer lamellae, while at longer exposure ultrasound induced the erosion of the inner lamellae, leading to an increase of amylose and the amorphous phase. These would explain the different behavior observed in sonication at treatment time ≥5 min. Solubility is negatively correlated to amylose content. Higher amylose content leads to a more compact gel structure, and it becomes more difficult to the soluble compounds to overflow outside the granules, resulting in lower solubility values (Seguchi, Hayashi, Suzuki, Sano, & Hirano, 2003; Yu, Ma, Menager, & Sun, 2012).

3.4. X-ray diffraction analysis

The X-ray diffraction patterns of native and treated samples are shown in Fig. 2. All samples show the typical A-type X-ray pattern for cereal starches, with characteristic peaks in 15, 17, 18, 23 and 26°; the reflection at 20º, which is usually connected with V-crystallinity, was also observed (Villanueva, Harasym, et al., 2018). The patterns obtained for treated samples showed a similar arrangement to the native flour, which could indicate that the crystallinity structure was not modified by ultrasound treatments. The main difference was a slight reduction in the diffraction intensities, especially in the case of CON-5 and TIM-60, the strongest conditions, seen in the shape and size of the characteristic peaks. Carmona-Garcia et al. (2016) also reported a greater reduction of diffraction intensities of different starches with increasing sonication time. However, the crystallinity of rice flour was not significantly affected by ultrasonication, with only TIM-2 presenting a lower value than the control. Yang et al. (2019) when sonicating rice starch at 150W reported a decrease, indicating that it was possible that it could be due to a damage to the amorphous regions rather than the crystalline region, since amorphous regions are more vulnerable to destruction by US. Kaur & Gill (2019) when sonicated rice starch at a frequency of 24 kHz for 15 and 30 min, concluded that the crystallinity remained unchanged, in agreement with the present study. Similar results were reported for other starches like corn (Amini et al., 2015; Flores-Silva et al., 2017; Luo et al., 2008)), taro and plantain (Carmona-García et al., 2016). It has been stated that the effect of

ultrasonication on the crystallinity content of starches depends on the type of starch, in addition to experimental conditions, since specific packing of crystalline and amorphous parts in the granule causes different susceptibilities to be attacked by ultrasounds, being found to promote an increase (Flores-Silva et al., 2017), decrease (Amini et al., 2015), or not promoting any significant change (Carmona-García et al., 2016; Luo et al., 2008).

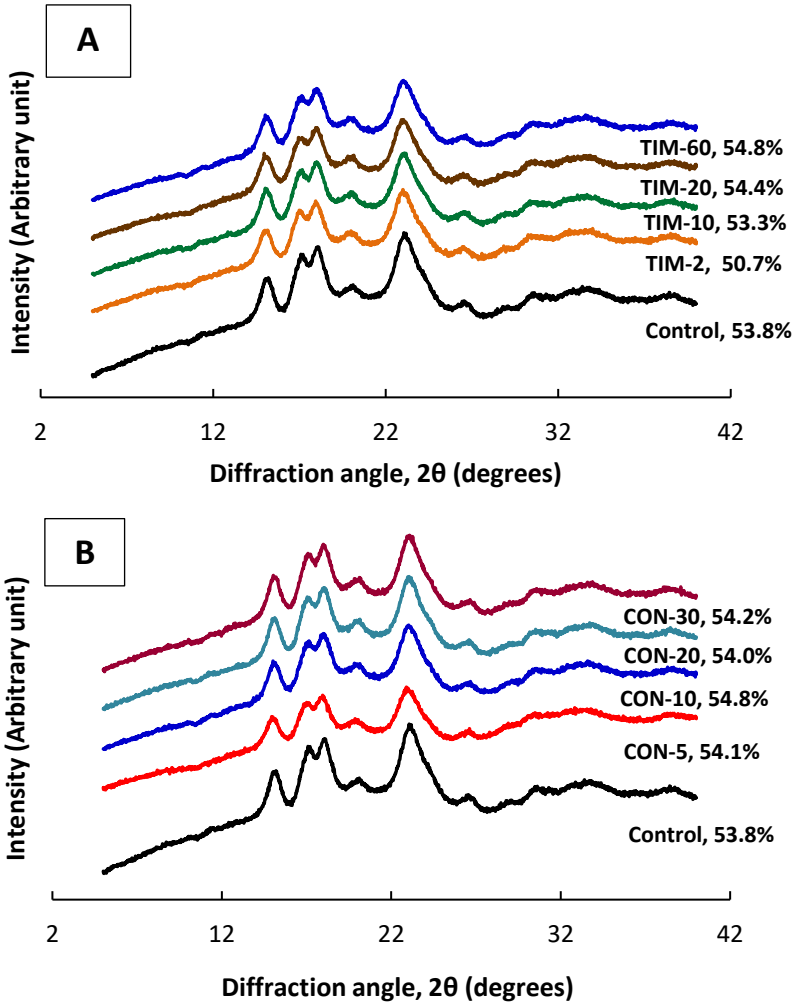

Figure 2. XRD pattern of control flour and flours treated at different time (A) and concentration (B). TIM-2, TIM-10, TIM-20; TIM-60, are samples sonicated for 2, 10, 20 and 60 min. CON-5, CON-10, CON-20 and CON-30: are samples sonicated at a flour concentration of 5, 10, 20 and 30 g/100 g dispersion. The crystallinity degree of each sample is indicated on the curve.

3.5. Fourier Transform Infrared Spectroscopy (FTIR)

FTIR spectra were studied in the region of 1200-900 cm^{-1}, for the analysis of short-range/double helical order of starch, and in the region of 1700-1600 cm^{-1}, for the study of proteins secondary structure of amide I band. The region of 1200-900 cm^{-1} is attributed to different types of transitions corresponding to carbohydrates, namely the C-C stretching vibrations (1200-1103 cm^{-1}) and the C-O bending vibrations (1047-994 cm^{-1}) (Bernazzani, Peyyavula, Agarwal, & Tatikonda, 2008; Ying et al., 2017). The band at 995 cm^{-1} is due to C-OH bending vibrations (particularly sensitive to water content in starch), while the bands at 1022 cm^{-1} and 1047 cm^{-1} are attributed to the amorphous and crystalline structures of starch, respectively (Bajer, Kaczmarek, & Bajer, 2013; Bernazzani et al., 2008; Man et al., 2012). The 1047/1022 ratio has been used to quantity the degree of short-range order in the starch, and is considered as an index of short-range crystallinity (Flores-Silva et al., 2017; Kaur & Gill, 2019; Wang et al., 2020), while the 1022/995 ratio gives information about the state of organization of the double helices located inside the crystallites (Monroy, Rivero, & García, 2018). The spectra of selected samples are shown in Fig. 3, as well as the obtained ratios of absorbance. In the case of 1047/1022 the control sample showed the highest result, significantly different than the sonicated samples, being 0.66 vs. 0.62-0.65. The 1022/995 ratio, on the other hand, showed the opposite trend, with the control showing the lowest value. This increase, however, does not show sharp changes nor follow an increasing trend with increasing exposure (Fig. 3). Similar results have been reported in sonicated rice (Yang et al., 2019) and cassava (Monroy et al., 2018) starch. Lower value of 1047/1022 ratio indicates lower relative crystallinity, while higher 1022/995 ratio refers to higher proportion of amorphous to ordered structure zones in starch granules (Kaur & Gill, 2019; Monroy et al., 2018). Flores-Silva et al. (2017) and Yang et al. (2019) agreed on this decreasing trend of the 1047/1022 ratio in sonicated-corn and rice starches respectively. They reported that the treatment of 4 min reached the lowest value and also agreed that longer exposure did not reflect additional changes in this ratio (Flores-Silva et al., 2017). The increase of the 1022/995 ratio indicates an increased proportion of short-chained amylose chains, which has been found to happen even at short exposure times, probably as a result of a disruption of amylose chains (Amini et al., 2015; Kaur & Gill, 2019). These results indicate that an increase can be quantified from sonication times as low as 2 min although no significant differences were obtained for sonication times longer than 10 min. In the case of varying flour concentration,

results show that an increase can be quantified even at the highest studied concentration of sonicated flour dispersion (CON-30).

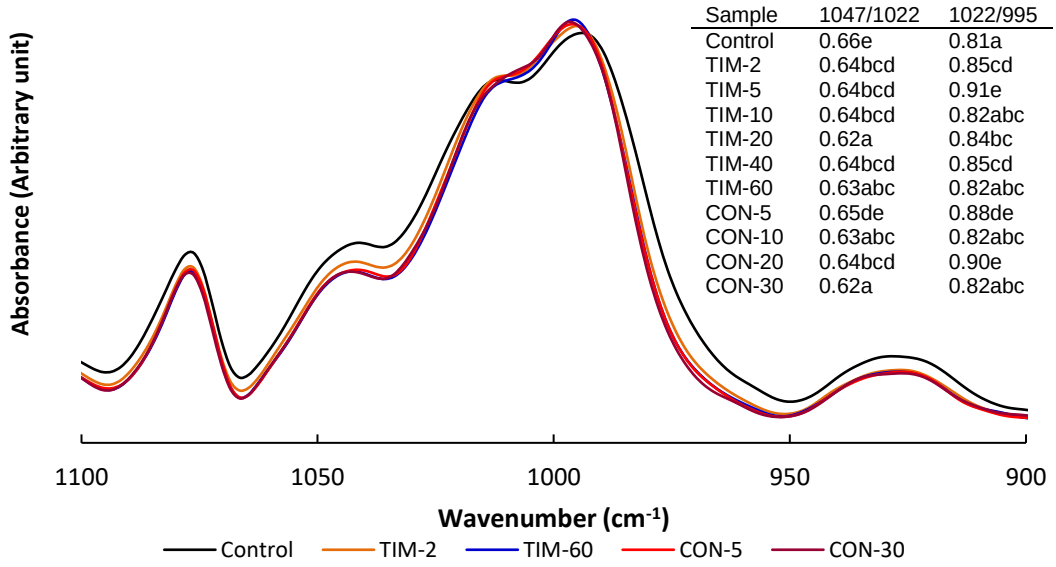

Sample	1047/1022	1022/995
Control	0.66e	0.81a
TIM-2	0.64bcd	0.85cd
TIM-5	0.64bcd	0.91e
TIM-10	0.64bcd	0.82abc
TIM-20	0.62a	0.84bc
TIM-40	0.64bcd	0.85cd
TIM-60	0.63abc	0.82abc
CON-5	0.65de	0.88de
CON-10	0.63abc	0.82abc
CON-20	0.64bcd	0.90e
CON-30	0.62a	0.82abc

Figure 3. FTIR spectra of selected samples, in the wavenumber range used to study changes in starch, with their respective 1047/1022 and 1022/995 ratio.

To estimate changes in secondary structure of proteins induced by ultrasonication, the interest was set in the range of 1700-1600 cm^{-1}, corresponding to amide I, the most prominent vibrational bands of the protein backbone structure (Kong & Yu, 2007; Ying et al., 2017). This band is due mainly to the C=O stretching vibration (~80%) of the amide groups coupled with some in-plane N-H bending (<20%) (Kong & Yu, 2007). Amide I band has been widely used to study protein folding, unfolding and aggregation with infrared spectroscopy due to its sensitivity to secondary structure of proteins (Barth, 2007). Changes in this band were estimated from the relative area of each individual peak (see Table 3). Fig. 4 shows the deconvolved curves of selected samples and the individual bands obtained according to second derivative peak identification. US treatments led to a significant reduction in α-helix and β-sheet structures up to 14% and 32% respectively in treated samples with regard to the native ones. The fraction of β-turn did not follow a clear trend, while random coil increased up to 52% as result of sonication. The decrease in α-helix (1658-1650 cm^{-1}) and β-sheet (1640-1600 cm^{-1}) structures had an improving effect on the random coil (1650-1640 cm^{-1}) structure after treatments, which suggests a rearrangement of polymeric subunits that leads

to an increase of the disordered structure, and indicates sensitivity of α-helix and β-sheet to ultrasonication. The differences in the secondary structure after ultrasonication are due to the shear forces of US mechanical action, disrupting the interactions between the protein molecules and influencing the protein molecule internal structure (X. Yang et al., 2017). A decrease of the intensity peaks (~1600cm^{-1}) has also been indicated after sonication of wheat and sweet potato flour (Cui & Zhu, 2020) and quinoa proteins (Vera, Valenzuela, Yazdani-Pedram, Tapia, & Abugoch, 2019) at a frequency of 20kHz. The amide I zone is altered by oscillations of the polypeptide structure, which could be caused by flexural vibration frequencies of the intra- and inter-molecular hydrogen bonds, as a consequence of the cavitation phenomenon (Vera et al., 2019).

Table 3. Protein secondary structure analysis of the studied samples.

	Protein secondary structure analysis (%)			
Sample	α-Helix	β-Sheet	β-Turn	Random coil
Effect of treatment time				
Control	21.6e	36.7e	20.8bc	21.0a
TIM-2	18.5a	36.1e	17.6a	27.8c
TIM-5	21.2de	33.4d	22.6ef	22.9b
TIM-10	19.2ab	31.5c	22.1de	27.4c
TIM-20	20.1bc	25.0a	23.1f	31.9d
TIM-40	19.0a	33.3d	20.1b	27.7c
TIM-60	20.5cd	27.8b	21.3cd	32.4d
SE	0.2	0.2	0.2	0.2
Analysis of variance and significance (p-values)				
	***	***	***	***
Effect of flour concentration				
Control	21.6c	36.7d	20.8d	21.0a
CON-5	23.5d	32.6c	14.1a	29.9c
CON-10	20.5b	27.8b	21.3d	32.4d
CON-20	19.5a	26.0a	19.2c	35.3e
CON-30	21.9c	33.0c	17.3b	27.9b
SE	0.2	0.2	0.2	0.2
Analysis of variance and significance (p-values)				
	***	***	***	***

SE: Pooled standard error from ANOVA. The different letters in the corresponding column within each studied factor indicate statistically significant differences between means at $p < 0.05$.
Analysis of variance and significance: *** $p < 0.001$. ** $p < 0.01$. * $p < 0.05$. ns: not significant.

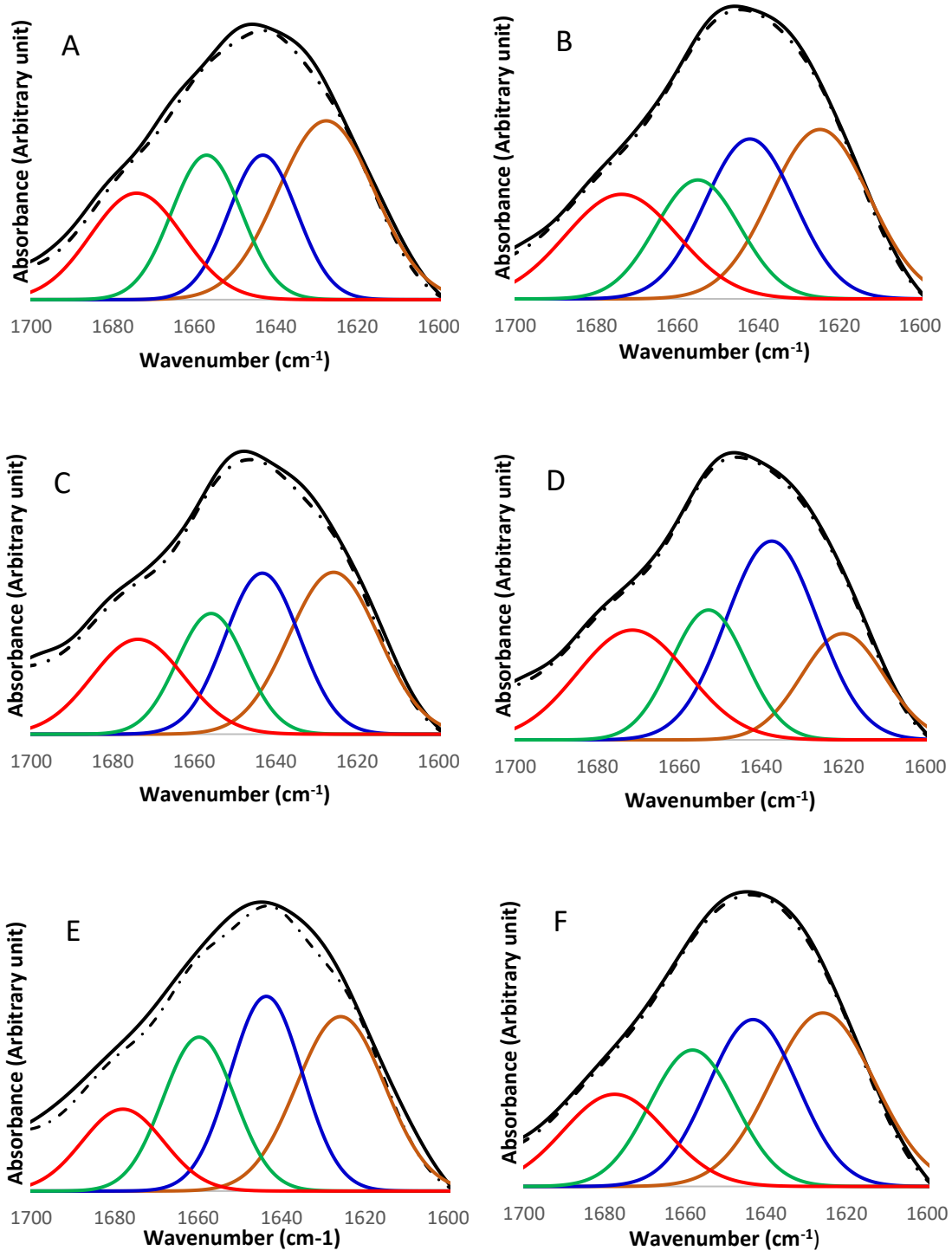

Figure 4. Deconvolved amide I bands of control and selected sonicated samples. A) Control; B) TIM-10; C) TIM-40; D) TIM-60 = CON-10; E) CON-5; F) CON-30. Deconvolved FTIR spectra are represented by a continuous line and the fitted curves by a discontinuous line. Bands: β-turns (1700-1660 cm^{-1}), α-helix (1658-1650 cm^{-1}), random coil (1650-1640 cm^{-1}) and β-sheet (1640-1600 cm^{-1}).

Table 4. Thermal properties of native and sonicated rice flour

Sample	First scan							Second scan					
	ΔH_{gel} (J/g)	$T_{O\text{-}gel}$ (°C)	$T_{P\text{-}gel}$ (°C)	$T_{E\text{-}gel}$ (°C)	ΔT (°C)	$\Delta H_{am\text{-}lip}$ (J/g)	$T_{P\text{-}am\text{-}lip}$ (°C)	ΔH_{ret} (J/g)	$T_{O\text{-}ret}$ (°C)	$T_{P\text{-}ret}$ (°C)	$T_{E\text{-}ret}$ (°C)	$\Delta H_{am\text{-}lip}$ (J/g)	$T_{P\text{-}am\text{-}lip}$ (°C)
Effect of treatment time													
Control	9.58b	61.1a	74.6c	81.5a	20.4d	1.4a	96.6a	4.3b	38.6a	51.4a	63.0bc	3.1a	98.2b
TIM-2	8.93a	61.1a	74.0a	79.7b	18.7c	1.8b	95.2a	3.4a	38.3a	51.1a	62.3ab	3.1a	97.0ab
TIM-5	8.76a	61.5a	74.2abc	80.0b	18.5bc	1.6ab	95.5a	3.9ab	38.0a	50.8a	61.9a	3.3a	96.6ab
TIM-10	9.02a	61.2a	74.18ab	79.3b	18.1abc	1.7ab	95.2a	3.5a	38.9a	51.5a	62.8abc	3.2a	97.0ab
TIM-20	9.00a	61.8a	74.2ab	79.3b	17.5a	2.0b	95.3a	3.4a	38.9a	53.1b	62.6abc	3.2a	96.3a
TIM-40	8.84a	61.6a	74.5bc	79.5b	17.9abc	2.0b	96.0a	3.7ab	38.1a	52.7b	61.8a	3.7b	96.7ab
TIM-60	8.94a	61.7a	74.4abc	79.5b	17.8ab	1.9b	96.3a	3.9ab	38.4a	50.7a	63.5c	3.2a	97.4ab
SE	0.13	0.2	0.1	0.3	0.2	0.1	0.4	0.1	0.5	0.2	0.2	0.1	0.4
Analysis of variance and significance (p-values)													
	**	ns	**	***	***	**	ns	**	ns	***	**	***	*
Effect of flour concentration													
Control	9.58c	61.1ab	74.6bc	81.5b	20.4b	1.4a	96.6a	4.3b	38.6a	51.4ab	63.0ab	3.1ab	98.2a
CON-5	9.23ab	61.3ab	74.3a	79.4a	18.1a	1.6ab	95.5a	4.1b	37.9a	50.9ab	62.7ab	2.7a	97.0a
CON-10	8.94a	61.7b	74.4ab	79.5a	17.8a	1.9bc	96.3a	3.9ab	38.4a	50.7a	63.5b	3.1ab	97.4a
CON-20	9.03a	60.9a	74.3a	79.5a	18.6a	1.7bc	96.4a	3.4a	37.8a	52.0b	62.7a	3.1ab	97.5a
CON-30	9.49bc	61.5ab	74.7c	79.9a	18.4a	2.0c	96.2a	3.7ab	37.4a	51.4ab	62.4a	3.3b	97.4a
SE	0.14	0.2	0.1	0.3	0.2	0.1	0.4	0.1	0.5	0.3	0.2	0.1	0.4
Analysis of variance and significance (p-values)													
	**	*	***	***	***	***	ns	**	ns	ns	*	*	ns

ΔH_{gel}: Enthalpy of gelatinisation. $To\text{-}_{gel}$, $T_{P\text{-}gel}$, $T_{E\text{-}gel}$: Onset, peak and endset temperatures of gelatinization. $\Delta T = (T_{E\text{-}gel} - To\text{-}_{gel})$. $\Delta H_{am\text{-}lip}$ = Enthalpy of the amylose-lipid complex dissociation. $T_{P\text{-}am\text{-}lip}$ = Peak temperature of the amylose-lipid complex dissociation. ΔH_{ret} = Enthalpy of melting of retrograded amylopectin. $T_{O\text{-}ret}$, $T_{P\text{-}ret}$, $T_{E\text{-}ret}$: Onset, peak, and endset temperatures of melting of retrograded amylopectin. ΔH_{gel}, ΔH_{ret}, $\Delta H_{am\text{-}lip}$ are given in J/g dry matter.

SE: Pooled standard error from ANOVA. The different letters in the corresponding column within each studied factor indicate statistically significant differences between means at $p < 0.05$. Analysis of variance and significance: *** $p < 0.001$. ** $p < 0.01$. * $p < 0.05$. ns: not significant.

3.6. Thermal properties

The thermal properties observed from the phase transitions detected from the gelatinization (first) and retrogradation (second) scans are summarized in Table 4. DSC thermograms of all samples showed two endothermic peaks, the main one associated to the starch gelatinization transition and a smaller peak caused by the amylose-lipid complex dissociation, appearing at the temperature range of 90-105ºC (Villanueva, Ronda, Moschakis, Lazaridou, & Biliaderis, 2018). Gelatinization enthalpy ΔH_{gel} was decreased after ultrasonication in all samples, from 9.58 J/g dm to 8.76-9.49 J/g dm. A similar behavior has been reported by Yang et al. (2019) when sonicating rice starch. Jambrak et al. (2010) stated that a decrease of the gelatinization enthalpy after ultrasonication possibly results from different alignments of hydrogen bonds within the starch molecules, as a consequence of the disruption of amorphous regions. The peak and endset gelatinization temperatures were decreased after sonication, while the onset gelatinization temperature was slightly increased. In all treated samples a narrowing of the gelatinization temperature range (ΔT) was determined, mainly due to a shift of $T_{E\text{-}gel}$ to significantly lower temperatures, going from 20.4°C, in the control, to up to 17.5°C at the more marked differences of time and concentration. Such reduction of ΔT, indicate a reinforcement of the starch structure after treatment probably because of a better packed crystalline leftovers structure after the breakage of amorphous regions and the melting of the weakest crystallites in the starch caused by cavitation (Amini et al., 2015; Chi et al., 2019; Luo et al., 2008). Even though an increase of $T_{O\text{-}gel}$ has been reported in several studies, the degree of said increase seems to vary depending mostly on the treatment conditions and treated matter, in this study the results obtained for sonicated samples were not found to be significantly different than the control (Carmona-García et al., 2016; Flores-Silva et al., 2017; Jambrak et al., 2010). Yang et al. (2019) did not report significant differences in the gelatinisation temperatures of rice starch after treatments at different sonication power levels, indicating that the range of modification achieved in $T_{P\text{-}gel}$ and $T_{E\text{-}gel}$ in this study could also be related to other components in the flour, not exclusively to starch. In the case of the amylose-lipid complex, the treatments significantly increased $\Delta H_{am\text{-}lip}$ values obtained from the first scan going from 1.4 J/g dm in native flour to 1.6-2.0 J/g dm in the treated samples, probably due to higher availability of amylose leaked outside the starch granule after the attack to the amorphous regions caused by sonication (Amini et al., 2015). The temperature of this transition was also lower in sonicated-flour samples (Table 4). The fact that no significant differences were observed between treated samples could be

explained as a degradation process limited by a minimum chain length in polymers, given that sonication breaks polymeric chains in a non-random manner, which could have been possibly achieved in 10 min of treatment (Czechowska-Biskup et al., 2005). To study the retrogradation enthalpy of amylopectin, a second scan was performed after 7 days of sample storage at 4°C. Two peaks were also found during the second scan, the first one, very wide, at a peak temperature of ~51°C, corresponding to the melting of recrystallized amylopectin, and the second one corresponding to the amylose-lipid complex dissociation (~97°C). The retrogradation enthalpy (~3.9 J/g dm) and temperatures obtained in the second scan were slightly modified by the treatments (Table 4). The enthalpy of the amylose-lipid complex dissociation obtained in the second scan was similar for all (native and sonicated) samples, and higher than in the first (gelatinization) scan. Eliasson (1994) reported that the increased values usually found during a second scan are probably due to better conditions for complex formation after the first heating because the leaking of amylose from granules can occur at temperatures above the gelatinization temperature range.

3.7. Pasting properties

The pasting parameters of studied flours are shown in Table 5. The pasting curves are shown in Figure 5. In flours, starch is the main component responsible for the development of pasting profiles. However, other components in rice flour also affect viscometric profiles, where proteins seem to play an important role (Meadows 2002). The results show that ultrasonication led to a decrease in the viscosity profile of rice flour during pasting. A similar effect was reported on ultrasonicated quinoa flour (Zhu & Li, 2019) and sweet potato starch (Zheng et al., 2013). Peak (PV), Breakdown (BV) and Setback viscosities (SV) were significantly decreased by ultrasound treatment. A decrease of PV could indicate that sonication weakens the granule structure (Chan, Bhat, & Karim, 2010). Lower PV values are usually related to an increased ratio of amylose to amylopectin in starch and to smaller granule size (Niu, Hou, & Zhao, 2017). Lower BV values after treatments indicate that the samples have a better capacity to withstand stress and heating than the control flour. The lower SV indicates a lower amylose retrogradation. BV was found to be significantly reduced with longer sonication time and higher concentration, up to -27% (TIM-60) and -32% (CON-30), for the lowest values obtained for each studied variable (Table 5). SV also followed an increasing reduction with longer treatment time, (-13% in TIM-60), and lower concentrations, (-14% in CON-5).

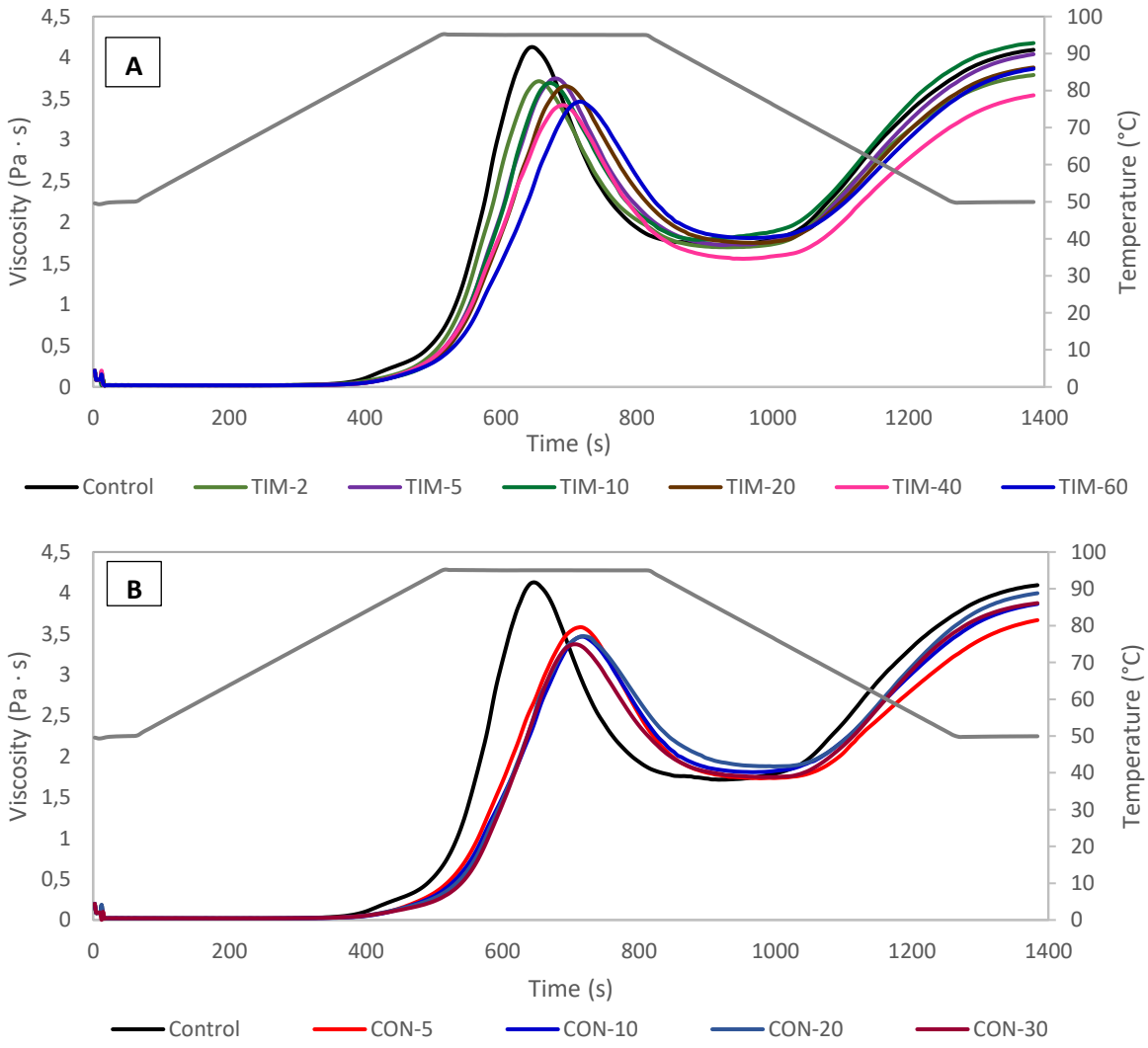

Figure 5. Pasting profile of native and treated flours at different (A) time and (B) concentration. The grey line corresponds to temperature (°C).

The pasting temperature (PT) was found to be significantly increased in all treated samples, which indicates that starch in rice flour was strengthened by the treatments as was observed from DSC assays. Opposite trend was reported by Yang et al (2019) in sonicated rice starch samples. They found increased viscometric profile and lower pasting temperatures in the treated samples with respect to native starch. The different effect of ultrasounds on rice starch and rice flour could be explained by the impact it has on rice proteins. As can be seen from FTIR spectra, proteins secondary structure was affected by US. Ultrasonication probably decreased proteins folding which would increase binding sites for binding water and other rice constituents. This would decrease the accessibility of water to granular components and reduce the rate and extent at which granular components leach out from the granule leading to lower pasting viscosities (Meadows, 2002). The increase in lipid-amylose complexation

extent observed just after gelatinization in sonicated samples from DSC could explain the decrease in the amylose available to retrograde and SV values in treated samples.

3.8. Rheological properties of gels made with sonicated rice flour

The rheological properties of gels made from sonicated rice flour were determined and compared to those of the gel made from the control/untreated flour by dynamic oscillatory tests. Table 5 presents the parameters obtained from fitting the power law model to the frequency sweeps data, and τ_{max} values and the stress at the crossing point (G'=G'' and tan δ=1) obtained from stress sweeps. The results showed that sonication increased τ_{max} in samples sonicated longer than 10 min and at concentrations above 20% reaching values up to 47% (TIM-10) and 56% (CON-30) higher than the native sample. This denotes sonicated samples led to stronger gel that resisted higher stress before its structure disruption. The stress at which gels go from a solid-like behavior to a viscous-like one (cross over, G'=G'') did not varied as result of sonication.

The oscillatory tests showed flour sonication had a significant impact on viscoelastic properties of gels. As can be seen in Table 5, although the elastic modulus, G_1', remained unaltered after sonication, the viscous one, G_1'', decreased up to -35% in both TIM-60 and CON-5 samples, with the concomitant decrease in (tan $\delta)_1$, that went from 0.17 to 0.11. These changes mean an increase in the relative predominance of the solid/elastic behavior of the gels (lower G''/G' ratio), while their consistency is decreased (equal G' and lower G''). This can be translated into softer gels that are able to maintain better their shape. Kaur & Gill (2019) when treating rice starch at high intensity ultrasound concluded that (tan $\delta)_1$ remains unchanged for treatment times below 30 min, while in rice flour significant differences were found in all studied sonication times, indicating that the other components found in flour play a decisive role in the samples' rheological properties. The decrease in the viscosity of the gels could be explained by the severe damage suffered by starch granules due to shear forces, causing the straightening out of amylose molecules resulting in a decrease of viscosity (Kaur & Gill, 2019). On the other side, the possible chains released from broken ramifications of amylopectin are unable to form a consolidated compact network during the gelatinization process (Carmona-García et al., 2016). Not many differences were found within treated samples, in agreement with the idea that the effect of ultrasonication has a disruption limit, as stated by Czechowska-Biskup et al. (2005), which in this study seems to happen in 10 minutes.

Table 5. Pasting parameters of studied samples.

Sample	PV (Pa · s)	FV (Pa · s)	TV (Pa · s)	PT (°C)	BV (Pa · s)	SV (Pa · s)	G_1' (Pa)	a	G_1'' (Pa)	b	tan $(\delta)_1$	c	τ_{max} (Pa)	Cross over (Pa)
Effect of treatment time														
Control	4.06d	4.15d	1.77a	80.2a	2.37d	2.37c	187a	0.092c	31c	0.342a	0.165d	0.250a	121a	175a
TIM-2	3.81c	4.06bcd	1.76a	82.4b	2.05c	2.30bc	169a	0.087bc	24ab	0.354b	0.138c	0.267ab	124a	166a
TIM-5	3.77c	4.08cd	1.74a	83.4cd	1.97c	2.36c	182a	0.084abc	25b	0.356bc	0.135bc	0.272abc	115a	166a
TIM-10	3.66b	4.13cd	1.75a	83.0bc	1.92bc	2.37c	191a	0.069ab	23ab	0.360bc	0.124abc	0.291bcd	179b	194a
TIM-20	3.61b	3.97bc	1.75a	83.5d	1.83ab	2.19b	201a	0.071ab	22ab	0.366c	0.117ab	0.295cd	174b	189a
TIM-40	3.48a	3.75a	1.71a	83.2cd	1.79a	2.06a	190a	0.064a	21ab	0.366bc	0.111a	0.302d	174b	192a
TIM-60	3.53a	3.87ab	1.80a	83.1c	1.73a	2.06a	174a	0.078abc	20a	0.367c	0.120abc	0.289bcd	147ab	174a
SE	0.02	0.05	0.04	0.2	0.04	0.04	9	0.005	1	0.003	0.005	0.006	12	7
Analysis of variance and significance (p-values)														
	***	***	ns	***	***	***	ns	**	***	***	***	***	***	*
Effect of flour concentration														
Control	4.06d	4.15c	1.77a	80.2a	2.37c	2.37c	187ab	0.092b	31c	0.342a	0.165b	0.250a	121a	175a
CON-5	3.53c	3.72a	1.72a	82.6b	1.83b	2.03a	167a	0.075ab	20a	0.363b	0.146b	0.288b	141ab	171a
CON-10	3.53c	3.87b	1.80a	83.1b	1.73b	2.06ab	174a	0.078b	20a	0.367b	0.120a	0.289b	147ab	174a
CON-20	3.45b	3.94b	1.80a	82.9b	1.71ab	2.10ab	191ab	0.073ab	23b	0.362b	0.119a	0.289b	178bc	188a
CON-30	3.37a	3.94b	1.79a	82.9b	1.60a	2.13b	205b	0.055a	22ab	0.365b	0.105a	0.310b	189c	204a
SE	0.02	0.04	0.03	0.2	0.04	0.02	8	0.006	1	0.004	0.005	0.009	12	9
Analysis of variance and significance (p-values)														
	***	***	ns	***	***	***	*	**	***	***	***	***	***	ns

PV = Peak Viscosity. FV = Final Viscosity. TV = Trough Viscosity. PT = Pasting Temperature. BV = Breakdown Viscosity. SV = Setback Viscosity.

G_1' (elastic modulus), G_1'' (viscous modulus) and tan $(\delta)_1$ (loss tangent) are the coefficients obtained from fitting the frequency sweeps data to power law model and represent the moduli and loss tangent values at a frequency of 1 Hz. The *a*, *b* and *c* exponents quantify the dependence degree of dynamic moduli and the loss tangent with the oscillation frequency. τ_{max} represents the maximum stress tolerated by the sample in the LVR.

SE: Pooled standard error from ANOVA. The different letters in the corresponding column within each studied factor indicate statistically significant differences between means at $p < 0.05$. Analysis of variance and significance: *** $p < 0.001$. ** $p < 0.01$. * $p < 0.05$. ns: not significant

4. Conclusion

Rice flour treated by ultrasounds at 24 kHz showed significant differences in functional, thermal, pasting and rheological properties. Physical differences could be observed at surface microstructure and particle size of treated samples, which define their interaction with water and, consequently, their pasting profile and rheological behavior. The thermal properties showed an important narrowing of gelatinization range, indicating a reinforced starch structure, probably because of a better packed crystalline leftovers structure. The information showed by XRD and the intensity ratios calculated using the FTIR spectra indicate a disruption of the outer branches of amylopectin chains due to sonication. FTIR also confirmed the modification of proteins secondary structure with the decrease in α-helix and β-sheet structures in benefit of the random coil structure. These molecular changes would explain the lower pasting profiles and increased PT obtained in treated samples. Rheological properties revealed that ultrasonication leads to softer gels but with higher elastic behavior. The results showed that the effect of ultrasonication does not highly depend on the concentration of the flour during the treatment within the studied range, which would make it advisable to use the highest concentration studied, 30%. On the other hand, the effect of time was detectable only up to 10 minutes; beyond this point not many differences were found. It can be concluded that ultrasound is a feasible technique for physically modify rice flour that would allow to tailor-make and improve its functional properties.

Acknowledgement

The authors thank the financial support of the Ministerio de Economía y Competitividad and the European Regional Development Fund (FEDER) (AGL2015-63849-C2-2-R), the Ministerio de Ciencia e Innovación (PID2019-110809RB-I00) and the Junta de Castilla y León/FEDER VA072P17. A. Vela thanks the Junta de Castilla y León for the doctorate grant and M. Villanueva thanks the Alfonso Martín Escudero Foundation for the post-doctoral grant.

References

AACC. (2014). AACC International methods, 76-31.01. Determination of Damaged Starch-Spectrophotometric Method. *AACC International Approved Methods*. https://doi.org/10.1094/aaccintmethod-76-31.01

AACC. (2017). AACC International methods, 76-21.02. General Pasting Method for Wheat or Rye Flour or Starch Using the Rapid Visco Analyser. *AACC International Approved Methods*, (11th Edition). https://doi.org/https://doi.org/10.1094/AACCIntMethod-76-21.01

Abebe, W., Collar, C., & Ronda, F. (2015). Impact of variety type and particle size distribution on starch enzymatic hydrolysis and functional properties of tef flours. *Carbohydrate Polymers*, *115*, 260–268. https://doi.org/10.1016/j.carbpol.2014.08.080

Amini, A. M., Razavi, S. M. A., & Mortazavi, S. A. (2015). Morphological, physicochemical, and viscoelastic properties of sonicated corn starch. *Carbohydrate Polymers*, *122*, 282–292. https://doi.org/10.1016/j.carbpol.2015.01.020

Ashokkumar, M. (2015). Applications of ultrasound in food and bioprocessing. *Ultrasonics Sonochemistry*, *25*(1), 17–23. https://doi.org/10.1016/j.ultsonch.2014.08.012

Bai, W., Hébraud, P., Ashokkumar, M., & Hemar, Y. (2017). Investigation on the pitting of potato starch granules during high frequency ultrasound treatment. *Ultrasonics Sonochemistry*, *35*, 547–555. https://doi.org/10.1016/j.ultsonch.2016.05.022

Bajer, D., Kaczmarek, H., & Bajer, K. (2013). The structure and properties of different types of starch exposed to UV radiation : A comparative study. *Carbohydrate Polymers*, *98*, 477–482.

Barth, A. (2007). Infrared spectroscopy of proteins. *Biochimica et Biophysica Acta - Bioenergetics*, *1767*(9), 1073–1101. https://doi.org/10.1016/j.bbabio.2007.06.004

Bel Haaj, S., Magnin, A., Pétrier, C., & Boufi, S. (2013). Starch nanoparticles formation via high power ultrasonication. *Carbohydrate Polymers*, *92*(2), 1625–1632. https://doi.org/10.1016/j.carbpol.2012.11.022

Bernazzani, P., Peyyavula, V. K., Agarwal, S., & Tatikonda, R. K. (2008). Evaluation of the phase composition of amylose by FTIR and isothermal immersion heats. *Polymer*, *49*(19), 4150–4158. https://doi.org/10.1016/j.polymer.2008.07.022

Byler, D. M., & Susi, H. (1986). Examination of the secondary structure of proteins by deconvolved FTIR spectra. *Biopolymers*, *25*(3), 469–487. https://doi.org/10.1002/bip.360250307

Carmona-García, R., Bello-Pérez, L. A., Aguirre-Cruz, A., Aparicio-Saguilán, A., Hernández-Torres, J., & Alvarez-Ramirez, J. (2016). Effect of ultrasonic treatment on the morphological, physicochemical, functional, and rheological properties of starches with different granule size. *Starch/Staerke*, *68*(9–10), 972–979. https://doi.org/10.1002/star.201600019

Chan, H. T., Bhat, R., & Karim, A. A. (2010). Effects of sodium dodecyl sulphate and sonication treatment on physicochemical properties of starch. *Food Chemistry*, *120*(3), 703–709. https://doi.org/10.1016/j.foodchem.2009.10.066

Chemat, F., Zill-E-Huma, & Khan, M. K. (2011). Applications of ultrasound in food technology: Processing, preservation and extraction. *Ultrasonics Sonochemistry*, *18*(4), 813–835. https://doi.org/10.1016/j.ultsonch.2010.11.023

Chi, C., Li, X., Lu, P., Miao, S., Zhang, Y., & Chen, L. (2019). Dry heating and annealing treatment synergistically modulate starch structure and digestibility International Journal of Biological Macromolecules Dry heating and annealing treatment synergistically modulate starch structure and digestibility. *International Journal of Biological Macromolecules*, *137*(February 2020), 554–561. https://doi.org/10.1016/j.ijbiomac.2019.06.137

Cui, R., & Zhu, F. (2020). Effect of ultrasound on structural and physicochemical properties

of sweetpotato and wheat flours. *Ultrasonics Sonochemistry*, *6*, 105118. https://doi.org/10.1016/j.ultsonch.2020.105118

Czechowska-Biskup, R., Rokita, B., Lotfy, S., Ulanski, P., & Rosiak, J. M. (2005). Degradation of chitosan and starch by 360-kHz ultrasound. *Carbohydrate Polymers*, *60*(2), 175–184. https://doi.org/10.1016/j.carbpol.2004.12.001

Degrois, M., Gallant, D., Baldo, P., & Guilbot, A. (1974). The effects of ultrasound on starch grains. *Ultrasonics*, *12*(3), 129–131. https://doi.org/https://doi.org/10.1016/0041-624X(74)90070-5

Eliasson, A. C. (1994). Interactions between starch and lipids studied by DSC. *Thermochimica Acta*, *246*(2), 343–356. https://doi.org/10.1016/0040-6031(94)80101-0

Flores-Silva, P., Roldan-Cruz, C., Chavez-Esquivel, G., Vernon-Carter, E. J., Bello-Pérez, L. A., & Alvarez-Ramírez, J. (2017). In vitro digestibility of ultrasound-treated corn starch, *1700040*, 1–9. https://doi.org/10.1002/star.201700040

Huang, Q., Li, L., & Fu, X. (2007). Ultrasound Effects on the Structure and Chemical Reactivity of Cornstarch Granules. *Starch/Stärke*, *59*, 371–378. https://doi.org/10.1002/star.200700614

Iida, Y., Tuziuti, T., Yasui, K., Towata, A., & Kozuka, T. (2008). Control of viscosity in starch and polysaccharide solutions with ultrasound after gelatinization. *Innovative Food Science and Emerging Technologies*, *9*(2), 140–146. https://doi.org/10.1016/j.ifset.2007.03.029

Jambrak, A. R., Herceg, Z., Šubarić, D., Babić, J., Brnčić, M., Brnčić, S. R., … Gelo, J. (2010). Ultrasound effect on physical properties of corn starch. *Carbohydrate Polymers*, *79*(1), 91–100. https://doi.org/10.1016/j.carbpol.2009.07.051

Jitngarmkusol, S., Hongsuwankul, J., & Tananuwong, K. (2008). Chemical compositions, functional properties, and microstructure of defatted macadamia flours. *Food Chemistry*, *110*(1), 23–30. https://doi.org/10.1016/j.foodchem.2008.01.050

Kaur, H., & Gill, B. S. (2019). Effect of high-intensity ultrasound treatment on nutritional, rheological and structural properties of starches obtained from different cereals. *International Journal of Biological Macromolecules*, *126*, 367–375. https://doi.org/10.1016/j.ijbiomac.2018.12.149

Knorr, D., Zenker, M., Heinz, V., & Lee, D. U. (2004). Applications and potential of ultrasonics in food processing. *Trends in Food Science and Technology*, *15*(5), 261–266. https://doi.org/10.1016/j.tifs.2003.12.001

Kong, J., & Yu, S. (2007). Fourier Transform Infrared Spectroscopic Analysis of Protein Secondary Structures Protein FTIR Data Analysis and Band Assign-. *Acta Biochimica et Biophysica Sinica*, *39*(20745001), 549–559. https://doi.org/10.1111/j.1745-7270.2007.00320.x

Kumar, V., Sharma, H. K., & Singh, K. (2017). Effect of precooking on drying kinetics of taro (Colocasia esculenta) slices and quality of its flours. *Food Bioscience*, *20*(August), 178–186. https://doi.org/10.1016/j.fbio.2017.10.003

Luo, Z., Fu, X., He, X., Luo, F., Gao, Q., & Yu, S. (2008). Effect of ultrasonic treatment on the physicochemical properties of maize starches differing in amylose content. *Starch/Staerke*, *60*(11), 646–653. https://doi.org/10.1002/star.200800014

Man, J., Yang, Y., Zhang, C., Zhou, X., Dong, Y., Zhang, F., … Wei, C. (2012). Structural Changes of High-Amylose Rice Starch Residues following in Vitro and in Vivo Digestion. *Agricultural and Food Chemistry*, *60*, 9332–9341.

Meadows, F. (2002). Pasting process in rice flour using rapid visco analyser curves and first derivatives. *Cereal Chemistry*, *79*(4), 559–562. https://doi.org/10.1094/CCHEM.2002.79.4.559

Mir, N. A., Riar, C. S., & Singh, S. (2019). Structural modification of quinoa seed protein isolates (QPIs) by variable time sonification for improving its physicochemical and functional characteristics. *Ultrasonics - Sonochemistry*, *58*(April), 104700. https://doi.org/10.1016/j.ultsonch.2019.104700

Monroy, Y., Rivero, S., & García, M. A. (2018). Microstructural and techno-functional properties of cassava starch modified by ultrasound. *Ultrasonics - Sonochemistry*, *42*(November 2017), 795–804. https://doi.org/10.1016/j.ultsonch.2017.12.048

Niu, M., Hou, G. G., & Zhao, S. (2017). Dough rheological properties and noodle-making performance of non-waxy and waxy whole-wheat flour blends. *Journal of Cereal Science*, *75*, 261–268. https://doi.org/10.1016/j.jcs.2017.05.002

O'Sullivan, J. J., Park, M., Beevers, J., Greenwood, R. W., & Norton, I. T. (2017). Applications of ultrasound for the functional modification of proteins and nanoemulsion formation: A review. *Food Hydrocolloids*, *71*, 299–310. https://doi.org/10.1016/j.foodhyd.2016.12.037

Ronda, F., Villanueva, M., & Collar, C. (2014). Influence of acidification on dough viscoelasticity of gluten-free rice starch-based dough matrices enriched with exogenous protein. *LWT - Food Science and Technology*, *59*(1), 12–20. https://doi.org/10.1016/j.lwt.2014.05.052

Seguchi, M., Hayashi, M., Suzuki, Y., Sano, Y., & Hirano, H.-Y. (2003). Role of Amylose in the Maintenance of the Configuration of Rice Starch Granules. *Starch/Stärke*, *55*, 524–528. https://doi.org/10.1002/star.200300172

Sujka, M. (2017). Ultrasonic modification of starch – Impact on granules porosity. *Ultrasonics Sonochemistry*, *37*, 424–429. https://doi.org/10.1016/j.ultsonch.2017.02.001

Sujka, M., & Jamroz, J. (2013). Ultrasound-treated starch: SEM and TEM imaging, and functional behaviour. *Food Hydrocolloids*, *31*(2), 413–419. https://doi.org/10.1016/j.foodhyd.2012.11.027

Vera, A., Valenzuela, M. A., Yazdani-Pedram, M., Tapia, C., & Abugoch, L. (2019). Conformational and physicochemical properties of quinoa proteins affected by different conditions of high-intensity ultrasound treatments. *Ultrasonics Sonochemistry*, *51*(August 2018), 186–196. https://doi.org/10.1016/j.ultsonch.2018.10.026

Villanueva, M., Harasym, J., Muñoz, J. M., & Ronda, F. (2018). Microwave absorption capacity of rice flour. Impact of the radiation on rice flour microstructure, thermal and viscometric properties. *Journal of Food Engineering*, *224*, 156–164. https://doi.org/10.1016/j.jfoodeng.2017.12.030

Villanueva, M., Ronda, F., Moschakis, T., Lazaridou, A., & Biliaderis, C. G. (2018). Impact of acidification and protein fortification on thermal properties of rice, potato and tapioca starches and rheological behaviour of their gels. *Food Hydrocolloids*, *79*, 20–29.

https://doi.org/10.1016/j.foodhyd.2017.12.022

Wang, H., Yang, Q., Gao, L., Gong, X., Qu, Y., & Feng, B. (2020). Functional and physicochemical properties of flours and starches from different tuber crops. *International Journal of Biological Macromolecules*, *148*, 324–332. https://doi.org/10.1016/j.ijbiomac.2020.01.146

Wu, Y., Chen, Z., Li, X., & Wang, Z. (2010). Retrogradation properties of high amylose rice flour and rice starch by physical modification. *LWT - Food Science and Technology*, *43*, 492–497.

Yang, W., Kong, X., Zheng, Y., Sun, W., Chen, S., Liu, D., … Ye, X. (2019). Controlled ultrasound treatments modify the morphology and physical properties of rice starch rather than the fine structure. *Ultrasonics Sonochemistry*, *59*. https://doi.org/10.1016/j.ultsonch.2019.104709

Yang, X., Li, Y., Li, S., Olayemi, A., Ruan, S., Wang, Y., … Ma, H. (2017). Effects of ultrasound pretreatment with different frequencies and working modes on the enzymolysis and the structure characterization of rice protein. *Ultrasonics - Sonochemistry*, *38*, 19–28. https://doi.org/10.1016/j.ultsonch.2017.02.026

Ying, D. Y., Hlaing, M. M., Lerisson, J., Pitts, K., Cheng, L., Sanguansri, L., & Augustin, M. A. (2017). Physical properties and FTIR analysis of rice-oat flour and maize-oat flour based extruded food products containing olive pomace. *Food Research International*, *100*(July), 665–673. https://doi.org/10.1016/j.foodres.2017.07.062

Yu, S., Ma, Y., Menager, L., & Sun, D. (2012). Physicochemical Properties of Starch and Flour from Different Rice Cultivars. *Food and Bioprocess Technology*, *5*, 626–637.

Yu, S., Zhang, Y., Ge, Y., Zhang, Y., Sun, T., Jiao, Y., & Zheng, X. Q. (2013). Effects of ultrasound processing on the thermal and retrogradation properties of nonwaxy rice starch. *Journal of Food Process Engineering*, *36*(6), 793–802. https://doi.org/10.1111/jfpe.12048

Zhang, L., Pan, Z., Shen, K., Cai, X., Zheng, B., & Miao, S. (2018). Influence of ultrasound-assisted alkali treatment on the structural properties and functionalities of rice protein. *Journal of Cereal Science*, *79*, 204–209. https://doi.org/10.1016/j.jcs.2017.10.013

Zheng, J., Li, Q., Hu, A., Yang, L., Lu, J., Zhang, X., & Lin, Q. (2013). Dual-frequency ultrasound effect on structure and properties of sweet potato starch. *Starch/Staerke*, *65*(7–8), 621–627. https://doi.org/10.1002/star.201200197

Zhu, F. (2015). Impact of ultrasound on structure, physicochemical properties, modifications, and applications of starch. *Trends in Food Science and Technology*, *43*(1), 1–17. https://doi.org/10.1016/j.tifs.2014.12.008

Zhu, F., & Li, H. (2019). Modification of quinoa flour functionality using ultrasound. *Ultrasonics Sonochemistry*, *52*(November), 305–310. https://doi.org/10.1016/j.ultsonch.2018.11.027

Zuo, J. Y., Knoerzer, K., Mawson, R., Kentish, S., & Ashokkumar, M. (2009). The pasting properties of sonicated waxy rice starch suspensions. *Ultrasonics Sonochemistry*, *16*(4), 462–468. https://doi.org/10.1016/j.ultsonch.2009.01.002

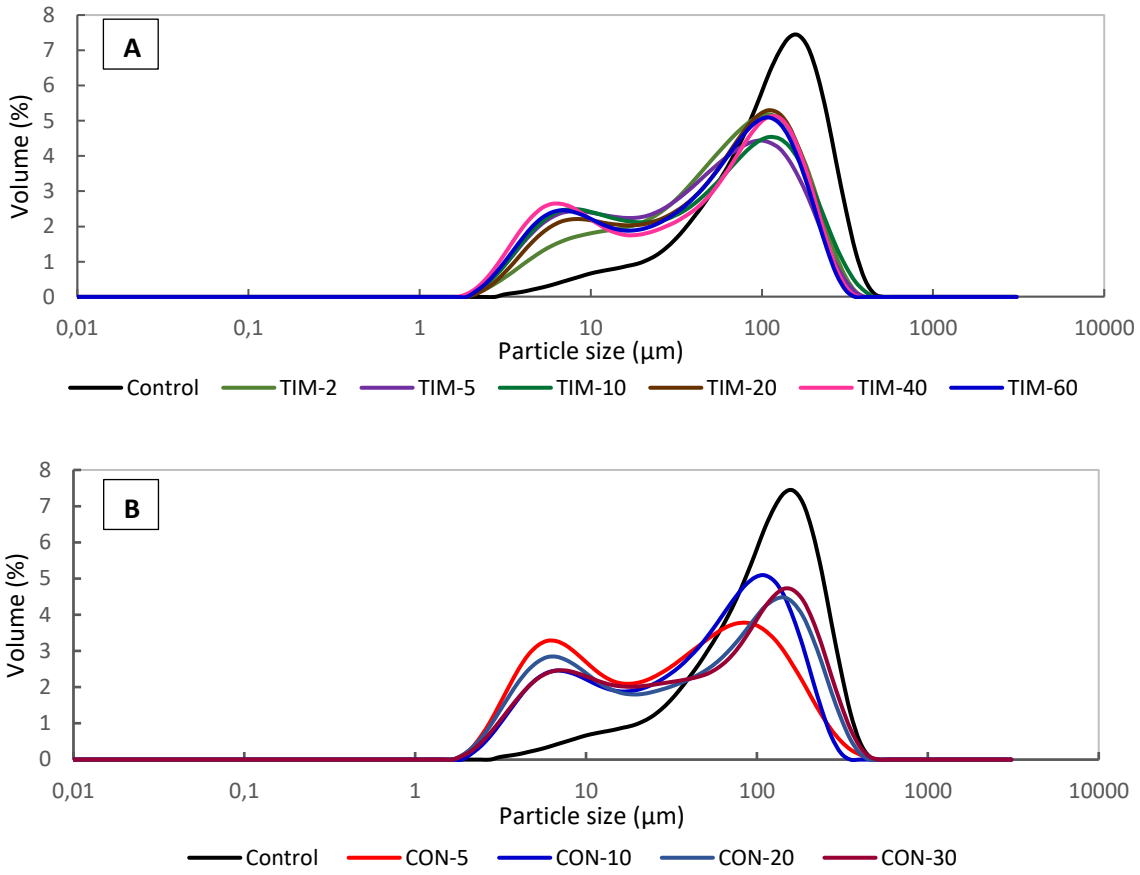

Supplementary Figure 1. Particle size distribution of native and ultrasonicated flour at different times (A) and at different flour concentration (B).